Dichroic Masers due to Radiation Anisotropy and the Influence of the Hanle Effect on the Circumstellar SiO Polarization

A. Asensio Ramos

Istituto Nazionale di Astrofisica (INAF) Osservatorio Astrofisico di Arcetri, Largo Enrico Fermi 5, 50125 Florence, Italy

E. Landi Degl'Innocenti

Dipartimento di Astronomia e Scienza dello Spazio, Largo Enrico Fermi 2, 50125 Florence, Italy

and

J. Trujillo Bueno[1]

Instituto de Astrofísica de Canarias, 38205, La Laguna, Tenerife, Spain

aasensio@arcetri.astro.it,landie@arcetri.astro.it,jtb@iac.es

ABSTRACT

The theory of the generation and transfer of polarized radiation, mainly developed for interpreting solar spectropolarimetric observations, allows to reconsider, in a more rigorous and elegant way, a physical mechanism that has been suggested some years ago to interpret the high degree of polarization often observed in astronomical masers. This mechanism, for which the name of "dichroic maser" is proposed, can operate when a low density molecular cloud is illuminated by an anisotropic source of radiation (like for instance a nearby star). Here we investigate completely unsaturated masers and show that selective stimulated emission processes are capable of producing highly polarized maser radiation in a non-magnetic environment. The polarization of the maser radiation is linear and is directed tangentially to a ring equidistant to the central star. We show that the Hanle effect due to the presence of a magnetic field can produce a rotation (from the tangential direction) of the polarization by more that 45° for some selected combinations of the strength, inclination and azimuth of the magnetic field

---

[1]Consejo Superior de Investigaciones Científicas, Spain

vector. However, these very same conditions produce a drastic inhibition of the maser effect. The rotations of about 90° observed in SiO masers in the evolved stars TX Cam by Kemball & Diamond (1997) and IRC+10011 by Desmurs et al. (2000) may then be explained by a local modification of the anisotropy of the radiation field, being transformed from mainly radial to mainly tangential.

Subject headings: magnetic fields — masers — polarization — stars: magnetic fields

1. Introduction

Growing attention has been devoted in recent years to the study of non-equilibrium phenomena involving populations of magnetic sublevels in astrophysical plasmas. Most of the work in this field has been carried out within the framework of the quantum theory of spectral line polarization and has been aimed at the physical understanding and numerical modeling of the scattering polarization phenomena observed in the radiation emitted by the outer layers of stellar atmospheres and, more particularly, of the solar atmosphere (Trujillo Bueno & Landi Degl'Innocenti 1997, Landi Degl'Innocenti 1998, 2003*a*, Trujillo Bueno 1999, 2001, 2003, Trujillo Bueno et al. 2002*a*, 2002*b*, 2004, Casini et al. 2002, Manso Sainz & Landi Degl'Innocenti 2002, Manso Sainz & Trujillo Bueno 2003, Landi Degl'Innocenti & Landolfi 2004).

Due mainly to limb darkening and to geometrical effects, the radiation field in the outer layers of stellar atmospheres is anisotropic and therefore capable of introducing differences in the populations of the magnetic sublevels (either degenerate or split by a magnetic field). These populations imbalances, in some cases accompanied by more complicated phenomena such as coherences –or quantum interferences– between different magnetic sublevels, are responsible for the appearance of polarization in the radiation emitted by the atoms (resonance polarization). The phenomenon of population imbalances between magnetic sublevels is well known in laboratory spectroscopy where it is often referred to as "atomic polarization" (Happer 1972). A low density plasma irradiated by a directional source of radiation –like for instance a nearby star– is the most appropriate physical environment where atomic polarization can play a fundamental role. This is because the atoms and/or molecules are irradiated by a highly anisotropic radiation field, whereas collisions with nearby particles are very sparse and are not capable of destroying the atomic polarization induced by the radiation.

In order to get a qualitative idea of the phenomena that we are going to address in

this paper, consider two atomic (or molecular) levels that are very close in energy like, for instance, two successive rotational levels of a particular vibrational state of a molecule, and suppose that the average population of the upper level (defined as the overall population divided by the statistical weight) is slightly smaller than the one of the lower level. In this situation, no masing action is possible according to the conventional view. But if a certain amount of atomic polarization is present either in the lower or in the upper level (or in both), it may well happen that *some magnetic sublevels of the upper level turn out to have a population larger than some magnetic sublevels of the lower level*, so that a particular kind of population inversion will exist between the two levels. This phenomenon will be referred to in the following as "selective population inversion". In this situation, masing action may become possible, though only between specific magnetic sublevels, and the result is that a radiation of a particular polarization character is amplified by stimulated emission, whereas radiation having a different polarization character is absorbed. A collection of atoms or molecules with selective population inversion thus behaves as a dichroic medium of a particular nature[1]. For this reason, we will refer to this kind of masing action as "dichroic masing". Phenomenological versions of this mechanism have indeed been invoked in the past to explain the large degree of polarization observed in astronomical SiO masers (Western & Watson 1983a, 1983b, 1984). Detailed calculations have been performed for the simplest transitions in saturated masers ($J = 1 \rightarrow 0$, $J = 2 \rightarrow 1$) and have led to interesting results.

Recent VLBA observations of SiO masers in the circumstellar environment of late-type stars have shown that the linear polarization of the SiO maser transitions is mainly tangential, i.e. in the direction parallel to a ring at a given distance to the central star (Kemball & Diamond 1997). These observations, complemented by further observations of circular polarization, were interpreted, using a formula by Elitzur (1996), as due to the presence of a strong magnetic field of ~ 10 G. Desmurs et al. (2000) noted that this magnetic field appears to be uncomfortably strong. They also noted that Kemball & Diamond (1997) found difficulties for defining a topological distribution of magnetic fields which was able to explain the tangential polarization. By means of a phenomenological approach, Desmurs et al. (2000) suggest that the radiative pumping mechanism can easily explain the tangential polarization observed in the SiO maser spots as a result of the anisotropic radiation field coming from the star which is illuminating the spot, even in the absence of magnetic fields. This mechanism, based on the assumption of a difference in the pumping rates for the different magnetic sublevels, was first proposed, though in a phenomenological way, by Bujarrabal &

---

[1]A medium is said to be dichroic when its absorption coefficient depends on the polarization of the incident radiation. In our case, the concept of dichroism can be generalized to allow also for stimulated emission effects.

Nguyen-Q-Rieu (1981) and later investigated in detail by Western & Watson (1983a, 1983b). Even more interesting is the fact that the observations by Kemball & Diamond (1997) show some SiO maser spots in which the polarization direction is almost radial instead of being tangential.

The quantum theory of polarization in spectral lines (see the monograph by Landi Degl'Innocenti & Landolfi 2004) is capable of dealing with this topic in a more rigorous and elegant way. Here, we apply it to the investigation of the polarization properties of the SiO maser lines in the unsaturated regime and of the mechanisms which may produce a rotation of the direction of polarization, i.e., the Hanle effect due to the presence of a magnetic field and/or a local variation of the anisotropy properties of the radiation field. Some of the results presented in this paper, in particular, those contained in Sec. 2.2 have been previously obtained by Litvak (1975) but we consider our formulation to be more rigorous. Moreover, it contains in a self-consistent manner all the physical mechanisms which may introduce population inequalities and coherences among the magnetic sublevels. These physical mechanisms are known (e.g., Western & Watson 1983a, 1983b) but they have always been treated in a phenomenological manner.

2. Basic equations

2.1. Polarized Radiative Transfer

Consider the propagation of a beam of polarized radiation through a medium which is optically active in the sense that its optical properties are such that they can generate and modify the polarization of the radiation. The propagation is described by the following radiative transfer equation (Landi Degl'Innocenti 1983):

$$\frac{d}{ds}\mathbf{I} = \epsilon - \mathbf{K}\mathbf{I}, \tag{1}$$

where $\mathbf{I} = (I, Q, U, V)^{\dagger}$ is the Stokes vector at the frequency and propagation direction under consideration (with $\dagger$ indicating the transpose of the vector), $\mathbf{K}$ is the 4×4 propagation matrix, $\epsilon = (\epsilon_I, \epsilon_Q, \epsilon_U, \epsilon_V)^{\dagger}$ is the emission vector in the four Stokes parameters and s is the geometrical distance along the ray. The $\mathbf{K}$ matrix contains contributions from both absorption and stimulated emission processes, which can be labeled as $\mathbf{K}^A$ and $\mathbf{K}^S$, respectively.

The explicit form of the matrix is the following:

$$\mathbf{K} = \mathbf{K}^A - \mathbf{K}^S = \begin{pmatrix} \eta_I & \eta_Q & \eta_U & \eta_V \\ \eta_Q & \eta_I & \rho_V & -\rho_U \\ \eta_U & -\rho_V & \eta_I & \rho_Q \\ \eta_V & \rho_U & -\rho_Q & \eta_I \end{pmatrix}, \tag{2}$$

where $\eta_I = \eta_I^{(A)} - \eta_I^{(S)}$, $\eta_Q = \eta_Q^{(A)} - \eta_Q^{(S)}$, $\cdots$. The propagation matrix $\mathbf{K}$ can also be written as

$$\mathbf{K} = \begin{pmatrix} \eta_I & 0 & 0 & 0 \\ 0 & \eta_I & 0 & 0 \\ 0 & 0 & \eta_I & 0 \\ 0 & 0 & 0 & \eta_I \end{pmatrix} + \begin{pmatrix} 0 & \eta_Q & \eta_U & \eta_V \\ \eta_Q & 0 & 0 & 0 \\ \eta_U & 0 & 0 & 0 \\ \eta_V & 0 & 0 & 0 \end{pmatrix} + \begin{pmatrix} 0 & 0 & 0 & 0 \\ 0 & 0 & \rho_V & -\rho_U \\ 0 & -\rho_V & 0 & \rho_Q \\ 0 & \rho_U & -\rho_Q & 0 \end{pmatrix}, \tag{3}$$

which helps to clarify that it has six contributions: three due to transitions from the lower level (l) to the upper level (u), and three due to the stimulated emission transitions from the upper level (u) to the lower level (l). Concerning the contributions of $l{\rightarrow}u$ transitions, we have *absorption* (the first matrix, $\mathbf{K}_1^A$, which is responsible for the attenuation of the radiation beam irrespective of its polarization state), *dichroism* (the second matrix, $\mathbf{K}_2^A$, which accounts for a selective absorption of the different polarization states), and *anomalous dispersion* (the third matrix, $\mathbf{K}_3^A$, which describes the dephasing of the different polarization states as the radiation beam propagates through the medium). Concerning the contributions of $u{\rightarrow}l$ stimulated transitions we have that $\mathbf{K}_1^S$ would be the amplification matrix (responsible for the amplification of the radiation beam irrespective of its polarization state), $\mathbf{K}_2^S$ would be the dichroism amplification matrix (responsible of a selective stimulated emission of different polarization states), and $\mathbf{K}_3^S$ would be the anomalous dispersion amplification matrix.

2.2. Dichroic Maser Condition

It can be shown that the eigenvalues of the propagation matrix are given by (see Landi Degl'Innocenti & Landi Degl'Innocenti 1985):

$$\lambda_1 = \eta_I - \Lambda_+, \qquad \lambda_{2,3} = \eta_I \pm \mathrm{i}\Lambda_-, \qquad \lambda_4 = \eta_I + \Lambda_+, \tag{4}$$

where i is the imaginary unit and

$$\Lambda_\pm = \sqrt{\frac{1}{2}\left[\sqrt{(\eta^2 - \rho^2)^2 + 4(\vec{\eta} \cdot \vec{\rho})^2} \pm (\eta^2 - \rho^2)\right]}, \tag{5}$$

and where we have introduced the formal vectors $\vec{\eta} = (\eta_Q, \eta_U, \eta_V)$ and $\vec{\rho} = (\rho_Q, \rho_U, \rho_V)$.

A dichroic maser can occur when at least one of the eigenvalues is negative (Landi Degl'Innocenti 2003b). Since the $\Lambda_\pm$ quantities are always non-negative, the smallest eigenvalue is $\eta_I - \Lambda_+$. This eigenvalue can become negative in the less restrictive conditions. When this condition is fulfilled, the particular mode of polarization associated with this eigenvalue (namely, an eigenvector of the **K** matrix) is exponentially amplified in the medium. It can be verified that this mode of polarization will be 100% polarized, when amplified, if the physical conditions in the medium remain constant and if the maser remains in the unsaturated regime. The transition to saturation is usually very fast, so that the optical depth is not so large as to permit one of the modes to completely dominate the radiation (Western & Watson 1984). The other eigenvalues can become negative under more restrictive conditions. The mode of polarization associated with λ_2 and λ_3 becomes amplified when $\eta_I < 0$ while that associated with λ_4 becomes amplified when $\eta_I + \Lambda_+ < 0$. In any case, the mode associated with the minimum eigenvalue, $\eta_I - \Lambda_+$, will be preferentially amplified.

In the usual case where polarization phenomena are neglected, the matrix **K** reduces to the identity matrix multiplied by the standard absorption coefficient (including the contribution from stimulated emission). Therefore, the quantities $\Lambda_\pm$ are zero and all the eigenvalues of the propagation matrix reduce to a single one, equal to η_I. In this case, the population inversion requirement is $\eta_I < 0$ so that the amplification is independent of the polarization mode of the radiation.

Consider an atomic system (atom or molecule) in an anisotropic environment having cylindrical symmetry around a given direction that we choose as the quantization axis of total angular momentum (the z-axis of our reference system). Consider the case where there is no magnetic field present in the medium. The populations of the single magnetic sublevels can be deduced by solving the statistical equilibrium equations for the multilevel atom case discussed in sections *7.1* and *7.2* of Landi Degl'Innocenti & Landolfi (2004). Such equations contain radiative rates and collisional rates due to collisions with the surrounding particles, whose velocity distribution can be considered, in a broad range of physical conditions, to be isotropic. It can be shown that, in such a physical environment, the atomic system can be described, using the formalism of the irreducible statistical tensors $\rho_Q^K(\alpha, J)$ (see, e.g., Landi Degl'Innocenti & Landolfi 2004), by the only elements with K even and $Q = 0$. Note that the statistical tensors can also be referred as the multipole components of the atomic density matrix. In this formalism, $\rho_0^0(\alpha, J)$ is proportional to the total population of the level with total angular momentum J, while $\rho_0^2(\alpha, J)$ is the so-called alignment coefficient. α is a collection of inner quantum numbers which include, among others, the vibrational quantum number. From now on, we will drop all the inner quantum numbers except for the

vibrational one, v, when needed. For instance, for a level with $J = 1$, one has:

$$\rho_0^0(J = 1) = (n_{-1} + n_0 + n_1)/\sqrt{3} \tag{6}$$

$$\rho_0^2(J = 1) = (n_{-1} - 2n_0 + n_1)/\sqrt{6}, \tag{7}$$

where n_M is the population of each magnetic sublevel $M = -1, 0, 1$.

Consider an electric dipole transition between two levels, the lower level (v_l, J_l) and the upper level (v_u, J_u). The elements of the propagation matrix $\mathbf{K}$ can be expressed in terms of the statistical tensors $\rho_0^K(v_l, J_l)$ which account for the absorption processes and $\rho_0^K(v_u, J_u)$ which account for the stimulated emission processes. The general expressions of the elements of the propagation matrix can be found in Landi Degl'Innocenti & Landolfi (2004), while the explicit expressions for the particular case of a line transition without overlapping with other lines can be found in Trujillo Bueno (2003). Consider the scattering geometry shown in Fig. 1. For a given direction $\mathbf{\Omega}$, passing through the atom or molecule and forming angles θ (polar angle, usually parameterized as $\mu = \cos\theta$) and χ (azimuth) with the quantization axis z, and defining the positive Q-direction in the plane $(z, \mathbf{\Omega})$ (vector $\mathbf{e}_1$ in the figure), all the elements of the propagation matrix are zero, except for η_I, η_Q and ρ_Q. This is valid for the zero magnetic field case that we are considering in this section. For this particular case, Λ_+ and Λ_- turn out to be simply given by $|\eta_Q|$ and $|\rho_Q|$, respectively. Therefore, the selective masing condition is

$$\lambda_1 = \eta_I - |\eta_Q| = \frac{h\nu_0}{4\pi}\mathcal{N}(2J_l + 1)B(J_l \to J_u)\left[a + b(3\cos^2\theta - 1) - 3|b|\sin^2\theta\right]\phi(\nu_0 - \nu) < 0, \tag{8}$$

where $\mathcal{N}$ is the number density of molecules, $B(J_l \to J_u)$ is the Einstein coefficient for absorption of the transition, and $\phi(\nu_0 - \nu)$ is the line profile centered at the transition frequency ν_0 and normalized to unity in frequency. The quantities a and b are given by:

$$a = \frac{\rho_0^0(J_l)}{\sqrt{2J_l + 1}} - \frac{\rho_0^0(J_u)}{\sqrt{2J_u + 1}}$$

$$b = \frac{1}{2\sqrt{2}}\left[w_{J_l J_u}^{(2)}\frac{\rho_0^2(J_l)}{\sqrt{2J_l + 1}} - w_{J_u J_l}^{(2)}\frac{\rho_0^2(J_u)}{\sqrt{2J_u + 1}}\right], \tag{9}$$

with the symbols $w_{J_l J_u}^{(2)}$ and $w_{J_u J_l}^{(2)}$ defined in Landi Degl'Innocenti (1984). Depending on the sign of b, the masing condition can be expressed as:

$$\begin{cases} a + 2b < 0 & \text{if } b < 0 \\ a + [3\cos(2\theta) - 1]b < 0 & \text{if } b > 0. \end{cases} \tag{10}$$

It can be verified that the direction of polarization of the emergent maser radiation is tangential to a ring at a given distance to the central star if $b < 0$, while it is perpendicular if $b > 0$. Of course, when $b = 0$, there is no atomic polarization, and the maser conditions transform into the usual condition $a < 0$. Finally, it is interesting to note that, even if $a > 0$, we can have a maser effect due to the presence of atomic polarization in the rotational levels, as already discussed in the Introduction.

2.3. SiO molecule

The results derived in the previous section can be applied to a simple SiO molecular model. This model represents the two lowest vibrational levels of SiO ($v = 0$ and $v = 1$) in the fundamental electronic state $X^1\Sigma^+$. The number of rotational levels included in the model does not need to be specified. For simplicity, we assume that the population of the energy levels of the fundamental vibrational level are in thermal equilibrium at a collisional temperature T_c and that the population of the rotational levels of the $v = 1$ vibrational level is due to the pumping of the stellar infrared radiation at 8 μm. The effect of collisions on the $v = 1$ levels is neglected.

Since the rotational levels of the lowest vibrational level are thermalized, the statistical tensors which describe the atomic polarization of these levels can be written as:

$$\rho_Q^K(v = 0, J_l) = \delta_{K0}\delta_{Q0}\rho_0^0(v = 0, J_l), \tag{11}$$

which states that all multipoles vanish except the one with $K = 0$ and $Q = 0$, which represents, apart from a factor, the overall population of the rotational level. They can be rewritten by using the Boltzmann law as

$$\rho_0^0(v = 0, J_l) = \frac{\sqrt{2J_l + 1}}{Z(T_c)} \exp[-E(v = 0, J_l)/T_c]. \tag{12}$$

$Z(T_c)$ is the partition function at the collisional temperature T_c and $E(v = 0, J_l)$ are the energies of the rotational levels.

The population and polarization state of the $v = 1$ levels are mainly driven by the vibro-rotational transitions, while the pure rotational transitions are merely anecdotic. Therefore, we only include in our model the vibro-rotational transitions. Since the electronic state has no spin and no orbital angular momentum, Hund's case (b) gives a very good approximation to the coupling of angular momenta in the SiO molecule. The Einstein coefficients for spontaneous emission can be written as:

$$A(v_u, J_u \to v_l, J_l) = A_0(2J_l + 1) \begin{pmatrix} J_u & J_l & 1 \\ 0 & 0 & 0 \end{pmatrix}^2, \tag{13}$$

where $A_0 = 6.61$ s^{-1} is the band integrated Einstein coefficient, obtained from Drira el al (1997). The statistical tensors $\rho_Q^K(v, J)$ of the rotational levels with $v = 1$ can be calculated by solving the statistical equilibrium equations (see Landi Degl'Innocenti 1984 for an example). We neglect stimulated emission produced by the infrared radiation coming from the star. This approximation is valid only if the number of photons per mode $(\bar{n})$ of the pumping radiation is very small.[2] Assuming a blackbody radiation for a central star with a temperature $T_\star = 2500$ K and affected by a geometrical dilution factor f due to the distance, we get:

$$\bar{n} = \frac{c^2}{2h\nu^3}B(T_\star)f, \tag{14}$$

which yields $\bar{n} < 0.1$ at 8 μm for distances of the order or larger than 2 stellar radii. Under such circumstances, the statistical equilibrium equations can be written as:

$$\frac{d}{dt}\rho_Q^K(v = 1, J_u) = \sum_{J_l}\sum_{K_lQ_l} T_A(JKQ, J_lK_lQ_l)\rho_{Q_l}^{K_l}(v = 0, J_l)$$
$$- \sum_{K'Q'} R_E(JKQ, K'Q')\rho_{Q'}^{K'}(v = 1, J_u) = 0, \tag{15}$$

where $T_A(JKQ, J_lK_lQ_l)$ and $R_E(JKQ, K'Q')$ are transfer and relaxation radiative rates whose expressions can be found in section *7.2.a* of Landi Degl'Innocenti & Landolfi (2004). Inserting in Eq. (15) the expressions for the radiative rates, after some Racah algebra we end up with the following expression:

$$\rho_0^K(v = 1, J_u) = \sum_{J_l} \frac{c^2}{2h\nu^3}\sqrt{(2J_l + 1)(2J_u + 1)}\begin{pmatrix} J_u & J_l & 1 \\ 0 & 0 & 0 \end{pmatrix}^2 w_{J_uJ_l}^{(K)}\rho_0^0(v = 0, J_l)J_0^K. \tag{16}$$

The quantities J_Q^K are the tensors of the radiation field at the wavelength of the infrared transition. Consider a plane-parallel layer in which the SiO molecules are present. We select the quantization axis along the radial direction, i.e., along the perpendicular to the slab. If the radiation field due to the star is unpolarized and axisymmetric around the quantization axis, the radiation field can be fully described with the following two tensors:

$$J_0^0 = \frac{1}{2}\int_{-1}^1 d\mu I(\mu) \tag{17}$$

$$J_0^2 = \frac{1}{4\sqrt{2}}\int_{-1}^1 d\mu\left[(3\mu^2 - 1)I(\mu)\right], \tag{18}$$

---

[2]When this is not the case, the main effect of stimulated emission is the one of reducing atomic polarization, mimicking the effect of a reduced anisotropy factor (see Landi Degl'Innocenti & Landolfi 2004, Section 10.9).

which are frequently parameterized in terms of the number of photons per mode, $\bar{n}$, and the anisotropy factor, w, defined by

$$\bar{n} = \frac{c^2}{2h\nu^3}J_0^0, \qquad w = \sqrt{2}\frac{J_0^2}{J_0^0}. \tag{19}$$

Note that the anisotropy factor is bounded in the interval $[-1/2, 1]$. Both extremes correspond to radiation predominantly directed perpendicularly to the symmetry axis of the radiation field and to radiation predominantly directed along the symmetry axis, respectively (e.g., the review by Trujillo Bueno 2001).

The expressions derived above allows us to investigate the conditions under which a dichroic maser appears in this simplified model of the SiO molecule. Let us assume for simplicity that we perform the observation at $\mu = 0$, which represents the geometry of a $90°$ scattering. This assumption is not so restrictive since this is precisely the geometry which maximizes the optical path of the maser radiation. In this extreme case, the maser conditions given by Eqs. (10) transform into $a + 2b < 0$ if $b < 0$ and $a - 4b < 0$ if $b > 0$.

Taking into account the properties of the symbols $w_{JJ'}^{(2)}$, it is easily verified that the quantity b has the opposite sign of w for transitions involving rotational levels with relatively low J values, while the quantity a is always positive. In the left panel of Figure 2 we show the variation of the ratio $-2b/a$ for each transition having an upper level J_u. This calculation has been obtained for $w = 1$ so that we have used the ratio $-2b/a$ to detect the masing transitions. The curves have been calculated with different values of the collisional temperature T_c. Note that, the higher the temperature, the larger the number of transitions which show selective population inversion. The dependence of the population inversion with J seems to follow the general observational results that the masers get weaker the higher the value of J in the $v = 1$ level (Jewell et al. 1987, Cernicharo et al. 1993, Bujarrabal 1994). Because the model we are investigating is completely radiative (except for the populations of the $v = 0$ vibrational level), we do not obtain a thermalization of the energy levels to this local temperature. The right panel of Figure 2 represents the results for a fixed temperature $T_c = 400$ K and for different values of w which span the allowed range. In this case, since we have positive and negative values of b, we have plotted the value of the masing condition appropriate in each case, i.e., $r = -2b/a$ if $b < 0$ and $r = 4b/a$ if $b > 0$. The first conclusion from this plot is that the masing conditions, although sensitive to the actual value of w, do not vary very much in the whole range of variation of the anisotropy factor. Of course, when $w = 0$ the radiation field is isotropic and we do not obtain a dichroic maser. The most important conclusion is that, since the polarization direction of the amplified radiation is dictated by the sign of b, *the variation of w represents the only mechanism to switch from maser radiation which is vibrating perpendicular to the quantization axis to radiation*

vibrating parallel to the quantization axis. The variation of any other parameter included in the model only changes the excitation state of the SiO rotational levels, but not the polarization of the amplified radiation.

3.   The influence of the Hanle effect

We now investigate the influence of a magnetic field on the atomic polarization of the rotational levels of the SiO molecules and on the polarization of the emergent radiation. This is nothing, but the so-called Hanle effect (see Trujillo Bueno 2001 for a recent review).

3.1.   Statistical tensors with a magnetic field

The presence in the maser formation region of a magnetic field inclined with respect to the symmetry axis of the pumping radiation field produces a symmetry breaking. As a result, the problem becomes much more complicated. Now the statistical tensors with $Q \neq 0$ have to be taken into account in order to have a correct description of the polarization state of the energy levels. The magnetic field $\mathbf{B}$ is oriented along a direction $\mathbf{\Omega}_B$ which, in general, does not coincide with the quantization axis (see Figure 1). However, in the reference system in which the quantization axis is chosen along the direction of the magnetic field, the statistical equilibrium equations are barely modified (see Section *7.2a* of Landi Degl'Innocenti & Landolfi 2004) and can be easily solved, obtaining:

$$[\rho_Q^K(v=1, J_u)]_{\text{mag}} = \frac{1}{1 + i\Gamma Q} \sum_{J_l} \frac{c^2}{2h\nu^3} \sqrt{(2J_l+1)(2J_u+1)} \begin{pmatrix} J_u & J_l & 1 \\ 0 & 0 & 0 \end{pmatrix}^2 \times$$

$$(-1)^Q w_{J_u J_l}^{(K)} \rho_0^0(v=0, J_l)[J_Q^K]_{\text{mag}}, \quad (20)$$

where we have explicitly indicated that this is valid only in the magnetic field reference frame. Since the tensors of the radiation field have also to be calculated in this same reference frame, we loose the cylindrical symmetry property and the tensor $[J_Q^K]_{\text{mag}}$ contains also terms with $Q \neq 0$. The effect of the magnetic field is to produce a reduction and a dephasing of the statistical tensors with $Q \neq 0$. This reduction and dephasing in the magnetic field reference frame depends on the function Γ which, in turn, depends on the magnetic field strength through the equation:

$$\Gamma = \frac{2\pi\nu_L g_L}{\sum_{J_l} A(J_u \to J_l)}, \quad (21)$$

where ν_L is the Larmor frequency which is proportional to the magnetic field strength and g_L is the Landé factor of the rotational level. The fundamental electronic level of SiO has neither spin nor electronic orbital angular momentum so that the Landé factor includes the contribution from the coupling between the magnetic field and the rotation of the nuclei and a further contribution from the coupling between the magnetic field and the rotation of the electronic cloud. For the level's Landé factor we have used the value $g_L = -8.365 \times 10^{-5}$ (Davis & Muenter 1974). In this case, being $\sum_{J_l} A(J_u \to J_l) \simeq 6.6~\text{s}^{-1}$, the magnetic field strength which leads to the critical value $\Gamma = 1$ is ~ 9 mG. This means that in the presence of a magnetic field of ~ 9 mG we should already expect a significant modification in the emergent linear polarization with respect to the zero field reference case[3].

For our purposes, it is however more appropriate to calculate the statistical tensors in the reference system in which the quantization axis is along the symmetry axis of the slab. In order to do so, we have to carry out a rotation of the original reference system by the Euler angles $(0, -\theta_B, -\chi_B)$, being θ_B and χ_B the angles which define the direction of the magnetic field with respect to the symmetry axis of the slab (see Figure 1). Taking into account the spherical tensor transformations under a rotation of the reference system, we obtain that the statistical tensors in the reference system with the quantization axis along the symmetry axis of the radiation field are given by the equation

$$[\rho_Q^K(v=1, J_u)]_{\text{rad}} = \sum_{J_l} \frac{c^2}{2h\nu^3} \sqrt{(2J_l+1)(2J_u+1)} \begin{pmatrix} J_u & J_l & 1 \\ 0 & 0 & 0 \end{pmatrix}^2 w_{J_u J_l}^{(K)} \rho_0^0(v=0, J_l) H_Q^{(K)}(\theta_B, \chi_B),$$
(22)

where

$$H_Q^{(K)}(B, \theta_B, \chi_B) = \sum_{Q'} \frac{1}{1+i\Gamma Q'} \sum_{Q''} [J_{-Q''}^K]_{\text{rad}} (-1)^{Q''} \mathcal{D}_{Q'Q}^{K}{}^*(-\theta_B, -\chi_B) \mathcal{D}_{Q'Q''}^{K}(-\theta_B, -\chi_B),$$
(23)

$\mathcal{D}$ being the usual rotation matrices (see, e.g., Edmonds 1960). We can simplify the previous equation taking into account that the pumping radiation field is unpolarized and has azimuthal symmetry, so that $J_Q^K = J_Q^K \delta_{Q0}$. In this case:

$$H_Q^{(K)}(B, \theta_B, \chi_B) = [J_0^K]_{\text{rad}} \sum_{Q'} \frac{1}{1+i\Gamma Q'} \mathcal{D}_{Q'Q}^{K}{}^*(-\theta_B, -\chi_B) \mathcal{D}_{Q'0}^{K}(-\theta_B, -\chi_B).$$
(24)

Furthermore, introducing the *magnetic kernel* $\mathcal{M}_{QQ'}^K(\vec{B})$ defined by Landi Degl'Innocenti &

---

[3]Actually, if B_c is the critical field, the sensitivity range of the Hanle effect lies between $0.1B_c$ and $10B_c$, approximately. For fields stronger than about $10B_c$ the emergent linear polarization is sensitive only to the orientation of the magnetic field vector, but not to its strength.

Landolfi (2004), the above expression can be written as:

$$H_Q^{(K)}(B, \theta_B, \chi_B) = \mathcal{M}_{Q0}^K(\vec{B})[J_0^K]_{\text{rad}}, \tag{25}$$

so that the statistical tensors when a magnetic field is present can be expressed in terms of those relative to the case with $B = 0$ through the equation

$$[\rho_Q^K(v = 1, J_u)]_{\text{rad}} = \mathcal{M}_{Q0}^K(\vec{B})[\rho_0^K(v = 1, J_u)]_{\text{B}=0}. \tag{26}$$

We can now use some of the relevant properties of the magnetic kernel in order to gain some information on the behavior of the statistical tensors when a magnetic field is included. Firstly, we can calculate the effect of a magnetic field on the ρ_0^0 statistical tensors. In this case, we have $\mathcal{M}_{00}^0 = 1$ because $\mathcal{D}_{Q'0}^0 = \delta_{Q'0}$. This result means that the presence of a magnetic field does not change the overall population of a rotational level J. Secondly, in the case of zero magnetic field we have to recover the original equations. Since the magnetic kernel transforms into δ_{Q0} in the limit $\Gamma = 0$, it can be proved that the equations are transformed immediately into the zero-field ones (as a consequence of the orthogonality of the rotation matrices). Finally, the dependence of $\mathcal{M}_{Q0}^K$ on the azimuth of the magnetic field (χ_B) is periodic, with a period which is proportional to Q. This can be proved by recalling the expression of the magnetic kernel in terms of the reduced rotation matrices (Landi Degl'Innocenti & Landolfi 2004):

$$\mathcal{M}_{Q0}^K(B, \theta_B, \chi_B) = e^{-i\chi_B Q} \sum_{Q''} \frac{1}{1 + i\Gamma Q''} d_{QQ''}^K(\theta_B) d_{Q''0}^K(-\theta_B). \tag{27}$$

Therefore, the tensors ρ_0^K are not modified when changing the azimuth of the magnetic field, and only the phase of those with $Q \neq 0$ vary periodically with χ_B.

From the previous equations, it is easy to see the effect of a magnetic field on the statistical tensors ρ_0^2, which can be written as:

$$[\rho_0^2(v = 1, J_u)]_{\text{rad}} = \left[[d_{00}^2(-\theta_B)]^2 + \frac{2}{1 + \Gamma^2}[d_{10}^2(-\theta_B)]^2 + \frac{2}{1 + 4\Gamma^2}[d_{20}^2(-\theta_B)]^2 \right] [\rho_0^K(v = 1, J_u)]_{\text{B}=0}. \tag{28}$$

Note from the previous expression that the factor between brackets, $\mathcal{M}_{00}^2$, is always non-negative for any value of the magnetic field vector, so that, there is no sign change in ρ_0^2 unless J_0^2 changes its sign. In Fig. 3 we plot the variation of $\mathcal{M}_{00}^2$ with the inclination of the magnetic field vector. Note that, when the magnetic field is zero or very small (small Γ) or when the magnetic field is along the symmetry axis of the radiation field ($\theta_B = 0$), the ρ_0^2 tensor is not modified. However, when the field increases until reaching the critical value $\Gamma = 1$, the quantity $\mathcal{M}_{00}^2$ decreases. When the field is very large, we get the asymptotic

curve labeled with $\Gamma = \infty$ in the plot, which is nothing but $[d_{00}^2(-\theta_B)]^2$. Note that ρ_0^2 goes to zero for a critical angle $\theta_{\rm crit} = 54.73°$, which is called Van Vleck's angle $(\cos^2\theta_{\rm crit} = 1/3)$. On the other hand, its asymptotical value becomes $1/4$ when $\theta_B = \pi/2$, i.e., when the field is perpendicular to the symmetry axis of the radiation field.

3.2. Maser condition

When a magnetic field is present, we have to take into account that η_U may be non-zero so that the eigenvalues are modified with respect to the non-magnetic case. Indeed, in this case, the quantity Λ_+ turns out to be given by $\sqrt{\eta_Q^2 + \eta_U^2}$. Since Λ_+ is always non-negative, even in the presence of a magnetic field, λ_1 (see Eq. (4)) is the smallest of the eigenvalues and the corresponding mode will be amplified the most. It is not easy to find a simple analytical formula for the eigenvalues since the expressions for η_I, η_Q and η_U have now contributions from ρ_Q^2, with $Q = 0, 1, 2$. However, if we take into account that the statistical tensors ρ_Q^K can be written in terms of the statistical tensors for zero magnetic field $[\rho_0^K]_{\rm B=0}$ times the $\mathcal{M}_{Q0}^K$ factors, it is possible to write expressions for the masing condition which are very similar to those obtained for the $B = 0$ case, namely:

$$\begin{cases} a + b\left(f_I + \sqrt{f_Q^2 + f_U^2}\right) < 0 & \text{if } b < 0 \\ a + b\left(f_I - \sqrt{f_Q^2 + f_U^2}\right) < 0 & \text{if } b > 0, \end{cases} \tag{29}$$

where b is calculated assuming no magnetic field (a is immune to the magnetic field in this simplified model). The quantities f_I, f_Q and f_U are combinations of the magnetic kernels $\mathcal{M}_{Q0}^2$ which depend on the orientation and strength of the magnetic field (B, θ_B and χ_B) and on the observation direction (θ and χ). Their explicit expressions can be found in App. A. It is important to note that in the magnetic case the azimuth χ of the observing direction with respect to the z axis becomes relevant and that, contrary to what happens in the zero field case, the quantity which gives the polarization state of the emerging radiation is the product bf_Q, instead of b.

Assuming an observation at $\mu = 0$ and $\chi = 0$, we have plotted in Figure 4 the variation of the factors $f_\pm = f_I \pm \sqrt{f_Q^2 + f_U^2}$ for different values of the strength and inclination of the magnetic field. When the magnetic field is very weak, we recover the already discussed maser conditions, that is, those given by Eqs. (10) with $\theta = \pi/2$. This result is, obviously, independent of the inclination of the magnetic field. When the field strength is increased until reaching the critical value $\Gamma = 1$ or larger, the maser conditions become more restrictive than in the zero-field case. This is true irrespectively of the sign of b because both f_+ and

f_- become smaller. The magnetic field produces an inhibition of the maser effect, leading to less inverted levels than in the zero-field case. Focusing on the case of the SiO maser lines with $b < 0$ ($w > 0$), a more restrictive limiting case appears for very inclined and strong fields for which the factor f_+ becomes negative. In this case, the maser mechanism has been completely inhibited and no rotational line can be inverted. If we consider now the results with $b > 0$ ($w < 0$) we see that f_- is always negative, except when the inclination of the field is around the Van Vleck angle. At this angle and for fields that are strong enough, an inhibition of the maser effect can occur. In the rest of cases, the maser is always active. Another interesting property is that, given an inclination of the magnetic field, a saturation effect in the maser condition is found when the strength of the field is increased. For example, when the magnetic field has an inclination of $\theta_B = \pi/4$, the factor f^+ saturates at $1/2$, one fourth of the value at $B = 0$. In the limiting case of $\Gamma \to \infty$, the expressions for f_I, f_Q and f_U simplify considerably because the magnetic kernel does not depend on the strength of the field (in fact, $f_U = 0$), so that f_+ and f_- only depend on the inclination and azimuth of the magnetic field and on the angles defining the line-of-sight. For $\mu = 0$, $\chi = 0$ and $\chi_B = 0$, we obtain:

$$f_+ = -1 + \frac{9}{2} \left[\cos^2 \theta_B - \cos^4 \theta_B \right] + \frac{3}{2} \sqrt{\cos^4 \theta_B \left(3 \cos^2 \theta_B - 1 \right)}$$
$$f_- = -1 + \frac{9}{2} \left[\cos^2 \theta_B - \cos^4 \theta_B \right] - \frac{3}{2} \sqrt{\cos^4 \theta_B \left(3 \cos^2 \theta_B - 1 \right)} \tag{30}$$

The behavior is similar to that shown in Figure 4 for $\log \Gamma = 2$. The quantity f_+ is positive for field inclinations below the Van Vleck angle, negative for inclinations above this critical angle and zero at the exact Van Vleck angle. Concerning f_-, it is always negative irrespective of the inclination of the field. Only for the Van Vleck angle we find $f_- = 0$.

In order to better represent the effect of a magnetic field on the maser condition, we show in Figure 5 similar plots to those of Figure 2. We have selected a collisional temperature T_c of 400 K and two different inclinations of the magnetic field, representative of the two different behaviors which can be seen in Figure 4. The left panel shows the results obtained when the inclination of the field is 45°. The case $\Gamma = 0$ is equal to that plotted in Figure 2 for $T_c = 400$ K. Note that, when the field is increased, the dichroic masers between the upper rotational levels of the $v = 1$ vibrational level are inhibited and, in the limit of very high magnetic fields, only the $J = 1 \to 0$ and $J = 2 \to 1$ transitions remain inverted. This is a direct consequence of the functional form of the f^+ quantity shown in Figure 4. On the other hand, on the right panel of Figure 5 we have shown the results for an inclination of 75°. In this case, when the field strength is increased, the transitions which present a dichroic maser rapidly reduce and for the case $\Gamma = 2$, we arrive to a situation in which the maser effect has been completely inhibited by the magnetic field.

The quantities which now dictate the polarization state of the emerging maser radiation are $\eta_Q \propto f_Q b$ and $\eta_U \propto f_U b$, where b is calculated assuming zero magnetic field. However, it is difficult to obtain information about the emergent linear polarization from the plots shown above, but we have to solve the transfer problem described by Eq. (1). Taking into account the expression of the propagation matrix, neglecting the spontaneous emission term (ϵ) and supposing that the elements of the propagation matrix are constant along the line of sight, the fractional linear polarization is given, in the general magnetic case, by:

$$Q/I = -\frac{\eta_Q}{\sqrt{\eta_Q^2 + \eta_U^2}} \tanh\left(s\sqrt{\eta_Q^2 + \eta_U^2}\right) \tag{31}$$

$$U/I = -\frac{\eta_U}{\sqrt{\eta_Q^2 + \eta_U^2}} \tanh\left(s\sqrt{\eta_Q^2 + \eta_U^2}\right). \tag{32}$$

When the ray proceeds through the masing region, both Q/I and U/I tend to an asymptotic value which is given by the ratio in front of the hyperbolic-tangent function. Recalling the dependence of η_Q and η_U on the quantities f_Q and f_U, the asymptotic fractional linear polarizations can be expressed as:

$$Q/I = -\frac{b}{|b|}\frac{f_Q}{\sqrt{f_Q^2 + f_U^2}} \tag{33}$$

$$U/I = -\frac{b}{|b|}\frac{f_U}{\sqrt{f_Q^2 + f_U^2}}. \tag{34}$$

The sign of the fractional linear polarization is then determined by the sign of f_Q and f_U and by the sign of b. Note that these expressions recover the sign of Q/I when there is no magnetic field. In this case, $f_U = 0$ and $f_Q = -3$ and Q/I has the same sign as b.

These expressions allow to determine the rotation angle of the linear polarization, defined by:

$$\alpha = \frac{1}{2}\arctan\left(\frac{U}{Q}\right) + \alpha_0, \tag{35}$$

where α_0 depends on the sign of Q and U (see, e.g., Landi Degl'Innocenti & Landolfi 2004). From Eqs. (33) and (34), we get

$$\alpha = \frac{1}{2}\arctan\left(\frac{f_U}{f_Q}\right) + \alpha_0, \tag{36}$$

We have shown in the left panel of Figure 6 the rotation angle when the strength and inclination of the magnetic field is changed while the azimuth of the field is set to $\chi_B = 0$.

When the field is weak the rotation angle is close to 90° irrespective of the value of its inclination, i.e., it is perpendicular to the axis of symmetry of the radiation field. Moreover, if the field inclination is lower than $\theta_B = 54.73°$ (the Van Vleck angle), the rotation angle is limited to 135° irrespective of the value of the field, meaning a rotation of only 45° with respect to the non-magnetic case. However, when the field increases and the inclination is above the Van Vleck critical angle, a rotation as large as 90° with respect to the non-magnetic case can be obtained. The magnetic field strength for obtaining this rotation should be larger than ∼90 mG which, in principle, seems quite reasonable. In the theoretical limit of $\Gamma \to \infty$, there is a sharp division between field inclinations below and above the Van Vleck angle. When the field inclination is below this critical angle, the polarization angle is 90°. When the inclination is larger than the Van Vleck angle, the polarization angle suddenly changes to 0°.

The right panel of Figure 6 shows the results when $\Gamma = 10$ and the inclination and azimuth of the field are changed. In this case, the rotation angle with respect to the non-magnetic case is larger than 45° only in two very small regions of the parameter space. One of them is found when the azimuth is close to zero (the same detected in the previous plot) and the other one is found for azimuths around 150° and inclinations of the order of 65°. This last region implies so restrictive conditions that we consider it not to be responsible for any observable rotation of the direction of polarization.

From the previous analysis, we have seen that there are several combinations of the magnetic field strength and direction (with respect to the radiation symmetry axis) which gives a rotation of the direction of polarization larger than 45°. Although this rotation could be, in principle, responsible for the rotation of the direction of polarization with respect to the tangential direction of ∼ 90° observed by Kemball & Diamond (1997), the necessary conditions are quite restrictive. Moreover, one can note from Figure 4 that these regions are quite coincident with those in which the maser action is completely inhibited by the presence of the magnetic field.

The investigation of the effect of a magnetic field on the SiO masers allows us to state that, at least under the assumptions we have made in this modeling, a rotation of more than 45° of the direction of polarization with respect to the non-magnetic case (i.e. the tangential direction) produced by a magnetic field is very improbable. In fact, this rotation is only obtained under very restricted conditions, which are moreover close to those inducing a complete inhibition of the maser due to the presence of the magnetic field. The necessity of this delicate combination of parameters comes from the fact that the magnetic field acts in a twofold way. On the one hand, it produces a rotation of the polarization angle that can attain very large values (∼ 90°) only when the inclination and strength of the field are

increased. On the other hand, the stronger and inclined the field, the larger the inhibition of the maser effect.

4. Anisotropy factor

The previous results suggest that the only effective way of producing a large rotation of the direction of polarization of the maser radiation with respect to the tangential direction is by a sign change in the anisotropy factor. In this section we calculate the anisotropy factor in a simple model in order to investigate under which conditions we can have this sign change.

Consider a slab of constant physical properties characterized by the source function S_0 which is illuminated by one side by a collimated and unpolarized radiation field I_0. This model represents the illumination properties of a slab in which the maser is located. The collimated illumination is playing the role of the radiation field coming from the star which, being quite far away from this region, can be considered to be point-like. Let the total optical depth of the slab be 2τ. In order to calculate the anisotropy factor at the central position of the slab, we have to solve the radiative transfer equation. Supposing that the illuminating radiation is unpolarized and that the physical conditions are constant in the slab, we can write the intensity for each angle $\mu = \cos\theta$ as:

$$I^+(\tau, \mu) = I_0 e^{-\tau/\mu}\delta(\mu - 1) + S_0\left(1 - e^{-\tau/\mu}\right) \qquad \mu > 0$$
$$I^-(\tau, \mu) = S_0\left(1 - e^{-\tau/|\mu|}\right) \qquad \mu < 0, \tag{37}$$

in which the $+$ superscript represents radiation propagating away from the star and the $-$ superscript represents radiation propagating towards the star. Note that the incoming illuminating radiation contributes only to the radiation with $\mu = 1$ because it is collimated. Once the specific intensity is obtained we can calculate the tensors of the radiation field given by Eq. (18) by performing analytically the required angular integrals to end up with the following formula for the anisotropy factor:

$$w = \frac{1}{2}\frac{(\tau^3 - 2\tau)E_1(\tau) - (\tau^2 - \tau - 2f)e^{-\tau}}{2 + 2\tau E_1(\tau) + (f - 2)e^{-\tau}}, \tag{38}$$

where $E_1(\tau)$ is the first exponential integral and $f = I_0/S_0$. Note that the anisotropy factor depends only on the total optical depth of the slab, τ, and on the ratio between the illuminating radiation field and the source function at the interior of the slab (I_0/S_0).

Fig. 7 shows the value of w for different configurations of the total optical depth of the slab and the ratio f. We have also indicated the curves of constant value of the anisotropy

factor. Note that there is a combination of τ and f in which the radiation field inside the slab is completely isotropic since $w = 0$. For the rest of combinations, we can find radiation fields inside the slab which are mainly radial ($w > 0$) or mainly tangential ($w < 0$). When the source function S_0 is more than ~ 4 times larger than the incident radiation field I_0, both positive and negative anisotropy factors are possible depending on the optical depth of the slab.

In view of the previous calculations, it is possible to have a change in the sign of the anisotropy factor by local perturbations of the physical properties of the medium. If the optical depth remains constant and the source function of the slab is increased (for example due to a local increase in the temperature), there is a transition from a radiation field which is mainly radial (produced by the illumination of the star) to a radiation field which is mainly tangential (produced by the self-illumination of the cloud). A similar conclusion was reached by Western & Watson (1983b) by investigating the SiO population inversion obtained with and without the presence of the stellar radiation field. On the other hand, if the temperature of the slab remains constant but the optical depth is increased, we can have a similar transition for a restricted set of ratios between the source function and the incoming radiation field. In case that the incoming radiation field is very strong, we will always get a radial radiation field (optically thin slab) or an isotropic field (optically thick slab).

5. Conclusions

We have shown that dichroic masing in the unsaturated regime can be considered a very efficient mechanism for producing highly polarized masers in diluted media. The nominal value of 100% for the polarization degree can however be attained only in idealized situations. In practice, it has to be expected that a number of different phenomena, like trapping of the pumping radiation, the presence of depolarizing collisions, the effect of saturation (that has been neglected here), and the variation of physical properties along the ray-path will cooperate in reducing the polarization degree.

Using a simple SiO model we have shown that the rotation of the direction of polarization observed in the maser transitions in circumstellar envelopes may be produced by the presence of a magnetic field or by a change in the anisotropy of the radiation field. The rotation due to the presence of an inclined and strong magnetic field is produced under quite restrictive conditions, since the magnetic field plays two different roles. On the one hand, it brings to a rotation of the direction of polarization. On the other hand, it produces a strong inhibition effect on the dichroic masers. The conditions under which the rotation of the direction of

polarization of the emerging radiation can be larger than 45° are almost equivalent to the conditions under which a complete inhibition of the maser effect is produced. Therefore, we consider that the magnetic field is hardly responsible of the observed rotations of the direction of polarization in circumstellar envelopes. The mechanism which we propose to produce such large rotations is a change of sign in the anisotropy factor. This change of sign may be produced by a local change in the physical properties of the slab (e.g., as a result of the presence of shock waves) so that the radiation illuminating the SiO molecules goes from mainly radial to mainly tangential. We have to remark, however, that in the saturated regime, a 90° rotation of the plane of polarization can indeed be obtained by a similar rotation of the magnetic field (Goldreich, Keeley & Kwan 1973) even for isotropic pumping.

A. Analytical expressions for f_I, f_Q and f_U

These are the quantities appearing in the maser condition when a magnetic field is present. Their analytical expressions are:

$$f_I = (3\mu^2 - 1)\mathcal{M}_{00}^2 - 2\sqrt{6}\mu\sqrt{1-\mu^2}\left(\cos\chi\mathrm{Re}\mathcal{M}_{10}^2 - \sin\chi\mathrm{Im}\mathcal{M}_{10}^2\right) + \tag{A1}$$

$$\sqrt{6}(1-\mu^2)\left(\cos 2\chi\mathrm{Re}\mathcal{M}_{20}^2 - \sin 2\chi\mathrm{Im}\mathcal{M}_{20}^2\right) \tag{A2}$$

$$f_Q = 3(\mu^2 - 1)\mathcal{M}_{00}^2 - 2\sqrt{6}\mu\sqrt{1-\mu^2}\left(\cos\chi\mathrm{Re}\mathcal{M}_{10}^2 - \sin\chi\mathrm{Im}\mathcal{M}_{10}^2\right) - \tag{A3}$$

$$\sqrt{6}(1+\mu^2)\left(\cos 2\chi\mathrm{Re}\mathcal{M}_{20}^2 - \sin 2\chi\mathrm{Im}\mathcal{M}_{20}^2\right) \tag{A4}$$

$$f_U = 2\sqrt{6}\sqrt{1-\mu^2}\left(\sin\chi\mathrm{Re}\mathcal{M}_{10}^2 + \cos\chi\mathrm{Im}\mathcal{M}_{10}^2\right) + 2\sqrt{6}\mu\left(\sin 2\chi\mathrm{Re}\mathcal{M}_{20}^2 + \cos 2\chi\mathrm{Im}\mathcal{M}_{20}^2\right). \tag{A5}$$

In these equations $\mu = \cos\theta$, and the angles θ (polar angle) and χ (azimuthal angle) specify the direction of observation with respect to the z-axis.
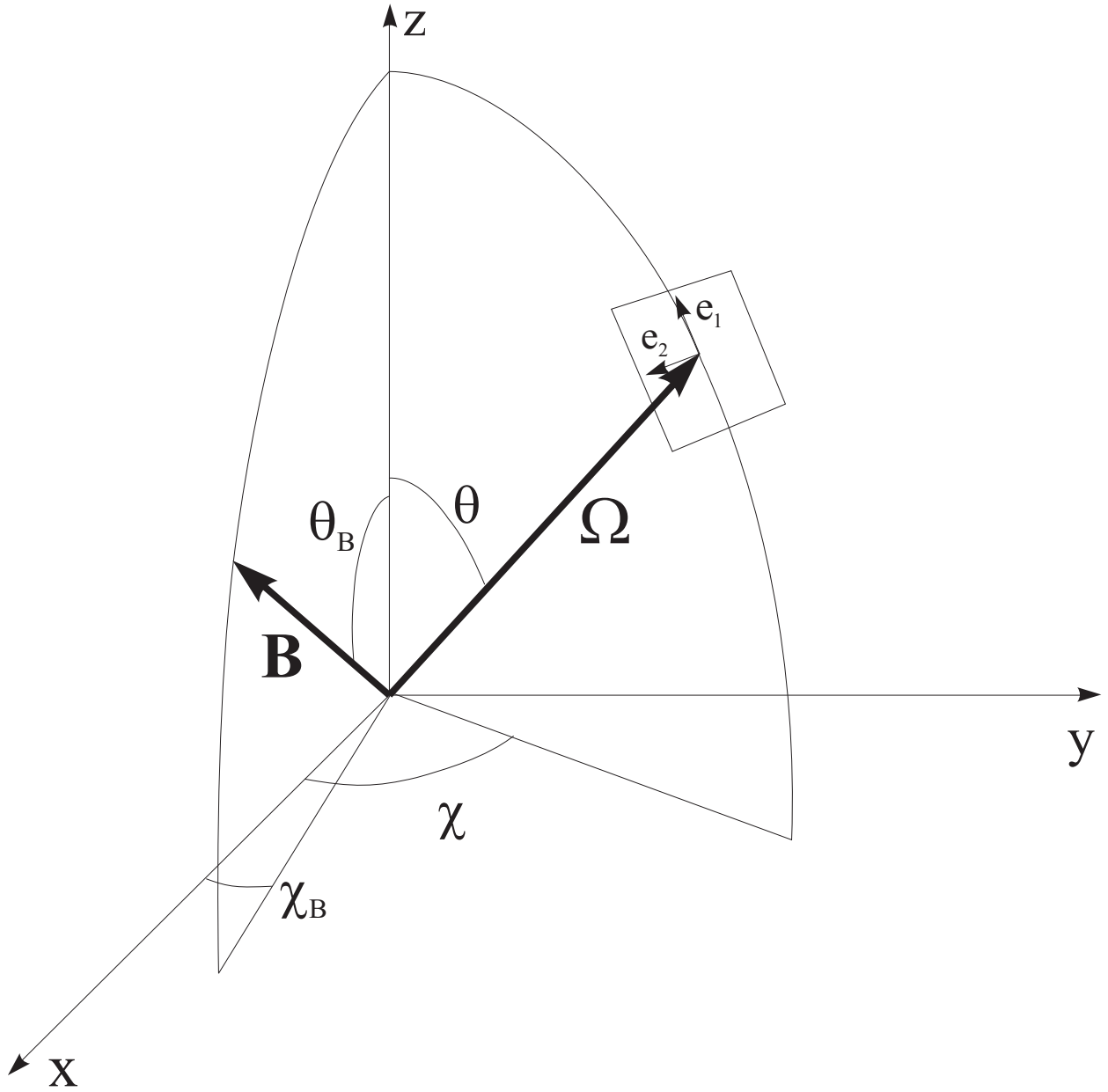
Fig. 1.— Scattering geometry indicating the quantization axis z, the direction of observation $\boldsymbol{\Omega}$ and the magnetic field vector $\mathbf{B}$. We have also indicated the unitary vectors $\mathbf{e}_1$ and $\mathbf{e}_2$, being the vector $\mathbf{e}_1$ the one that sets the reference direction for Stokes Q.
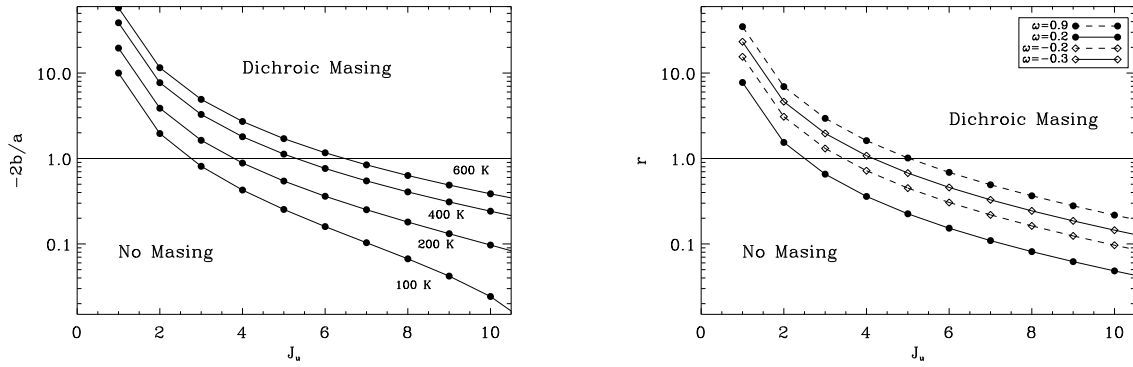
Fig. 2.— Maser condition for the rotational transitions inside the $v = 1$ vibrational level of SiO for the non-magnetic case for different values of the collisional temperature T_c (left panel) and for different values of the anisotropy factor w (right panel). The calculations of the left panel have been obtained with $w = 1$. The quantity which gives the maser condition when $b < 0$ (equivalent to $w > 0$ in the non-magnetic case) is $-2b/a$ while it is $4b/a$ when $b > 0$ (equivalent to $w < 0$ in the non-magnetic case). We designate this quantity as r in the right plot since we are plotting results with different values of w. The transitions are labeled with their upper total quantum number J_u. The number of inverted transitions increases when the collisional temperature is increased. It is interesting to note that the change of sign of the anisotropy factor does not destroy the dichroic maser in the lower rotational levels.
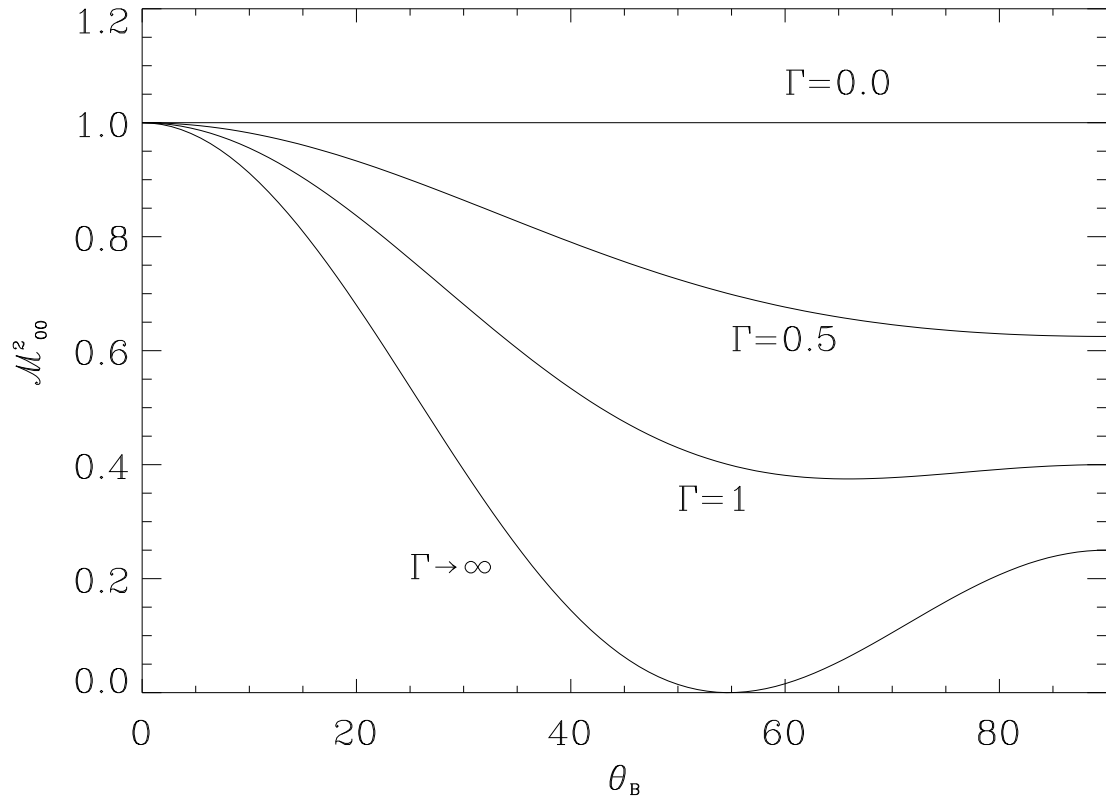
Fig. 3.— Variation of the function $\mathcal{M}_{00}^2$ with the inclination of the magnetic field for different values of the magnetic field intensity parameterized by the factor Γ.
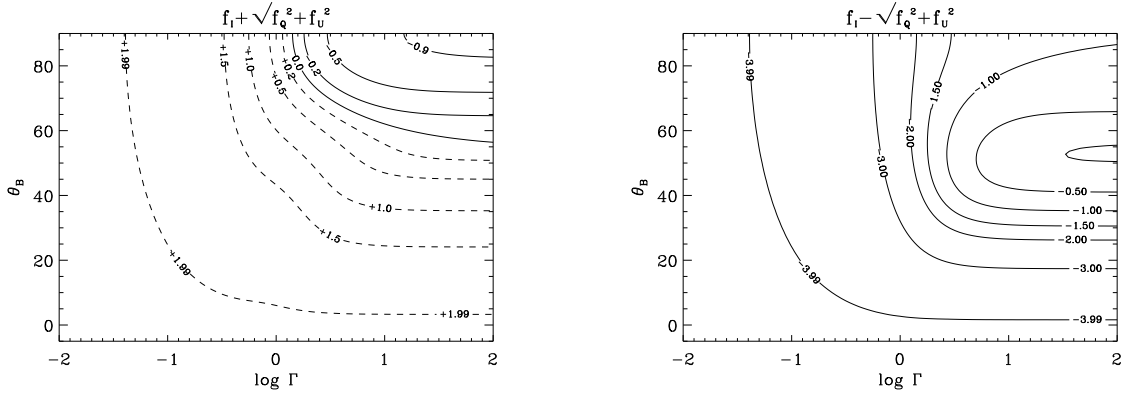
Fig. 4.— Dependence of the factors $f_{\pm} = f_I \pm \sqrt{f_Q^2 + f_U^2}$ with the strength and inclination of the magnetic field. When the magnetic field is very weak, we recover the original values given by Eqs. (10), namely, $f_+ \to 2$ and $f_- \to -4$ (using $\theta = \pi/2$). When the field is increased, the maser condition becomes more and more restrictive, until destroying any possibility of masing when the field is very large and inclined (because $a > 0$). For clarity, the isosurfaces with negative labels are plotted in solid lines, while those positive are plotted in dashed lines.
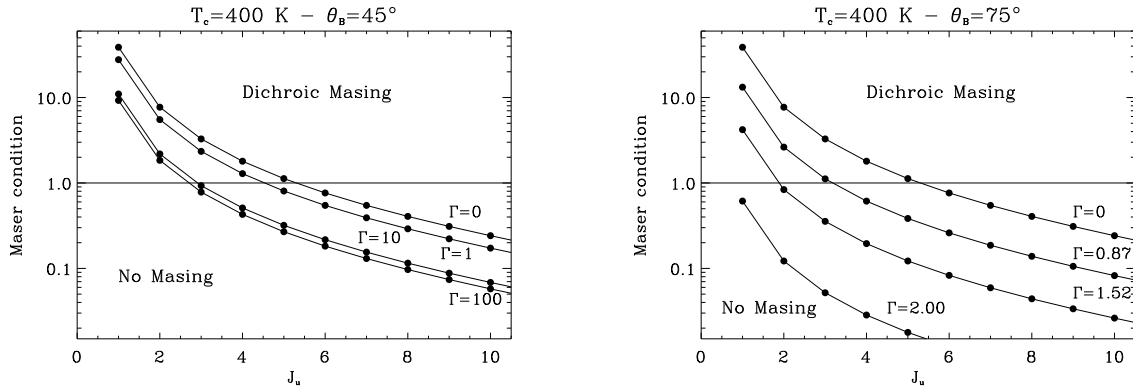
Fig. 5.— Maser condition for two values of the inclination of the magnetic field and different values of the strength of the field. The left panel shows that when the inclination is not very large ($\theta_B = 45°$, left panel) dichroic masers are possible in the lower rotational levels even when the magnetic field strength is very large. However, when the inclination is large ($\theta_B = 75°$, right panel), the dichroic maser can be completely destroyed by the magnetic field in all rotational levels. Both calculations have been obtained using $w = 1$.

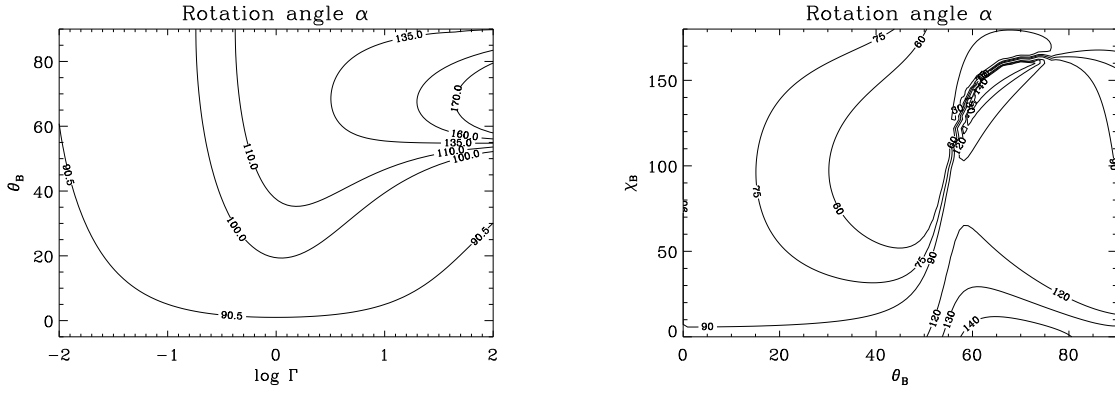Rotation angle α

Rotation angle α

Fig. 6.— Rotation angle defined in Eq. (35) for different combinations of the field strength and inclination, assuming $\chi_B = 0$ (left panel), and different combinations of the field inclination and azimuth, assuming $\Gamma = 10$ (right panel). When the magnetic field strength is very weak ($\Gamma \to 0$) or it is along the symmetry axis of the radiation field ($\theta_B = 0$) we recover the results obtained for the non-magnetic case, i.e., that the polarization of the observed light is perpendicular to the quantization axis.
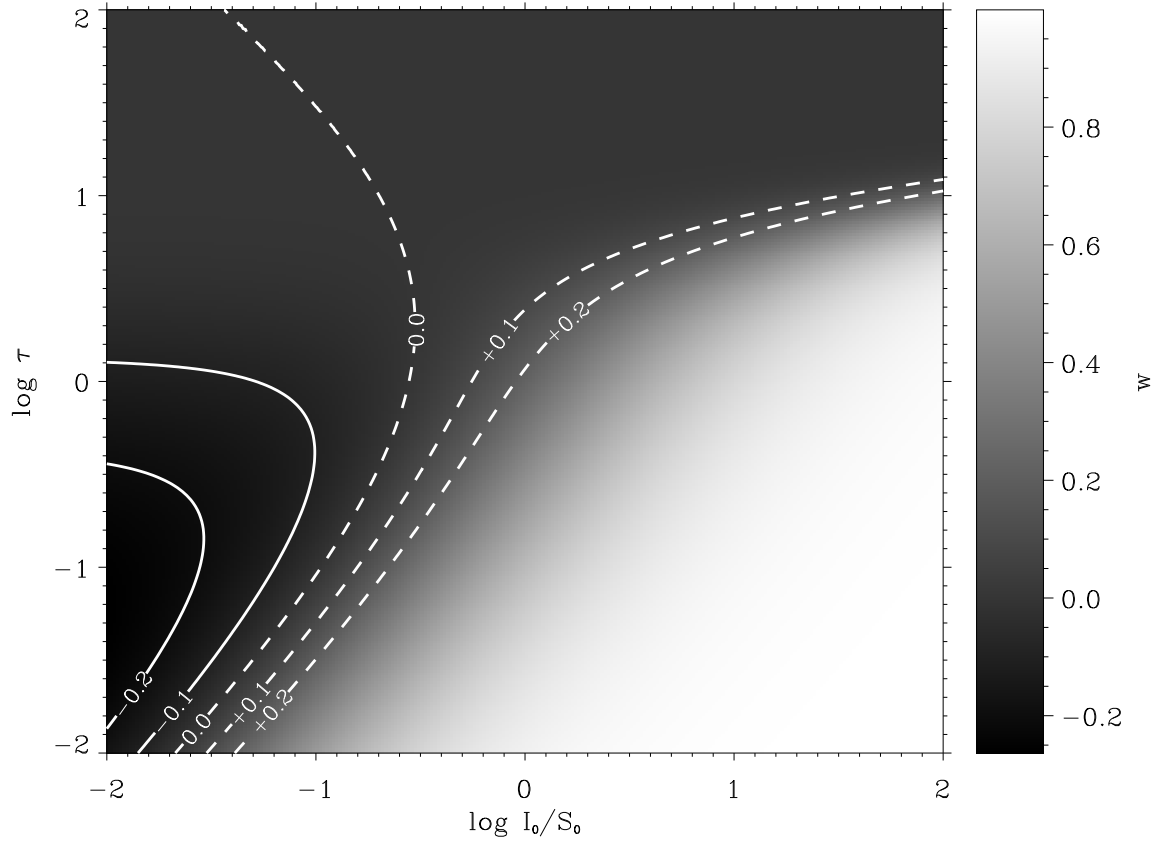
Fig. 7.— Anisotropy factor for different combinations of the total optical depth of the slab and the ratio I_0/S_0. For clarity, we have marked the position of $w = -0.2, -0.1$ with solid lines and the position of $w = 0.0, +0.1, +0.2$ with dashed lines.

REFERENCES

Bujarrabal, V. & Nguyen-Q-Rieu 1981, A&A, 102, 65

Bujarrabal, V. 1994, A&A, 285, 953

Casini, R., Landi Degl'Innocenti, E., Landolfi, M. & Trujillo Bueno, J. 2002, ApJ, 573, 864

Cernicharo, J., Bujarrabal, V., & Santarén, J. L. 1993, ApJ, 407, L33

Davis, R. E., & Muenter, J. S. 1974, J. Chem. Phys., 61, 2940

Desmurs, J. F., & Bujarrabal, V., & Colomer, F., & Alcolea, J. 2000, A&A, 360, 189

Drira, I., Huré, J. M., Spielfiedel, A., Feautrier, N., Roueff, E., 1997, A&A, 319, 720

Edmonds, A. R., Angular Momentum in Quantum Mechanics (Princeton University Press)

Eliztur, M. 1996, ApJ, 457, 415

Goldreich, P., Keeley, D. A., & Kwan, J. Y. 1973, ApJ, 179, 111

Happer, W. 1972, Rev. Mod. Phys., 44, 169

Jewell, P. R., Dickinson, D. F., Snyder, L. E., Clemens, D. P. 1987, ApJ, 323, 749

Kemball, A. J. & Diamond, P. J. 1997, ApJ, 481, L111

Landi Degl'Innocenti, E. 1982, Sol. Phys., 79, 291

Landi Degl'Innocenti, E. 1983, Sol. Phys., 85, 3

Landi Degl'Innocenti, E. 1984, Sol. Phys., 91, 1

Landi Degl'Innocenti, E. 1998, Nature, 392, 256

Landi Degl'Innocenti, E. 2003a, in *Solar Polarization 3*, eds. J. Trujillo Bueno & J. Sánchez Almeida, ASP Conf. Series, Vol. 307, 164

Landi Degl'Innocenti, E. 2003b, in *Astrophysical Spectropolarimetry*, eds. J. Trujillo Bueno, F. Moreno-Insertis & F. Sánchez, Cambridge University Press, 1

Landi Degl'Innocenti, E., & Landi Degl'Innocenti, M. 1985, Sol. Phys., 95, 239

Landi Degl'Innocenti, E., & Landolfi, M. 2004, Polarization in Spectral Lines (Kluwer Academic Publishers)

Litvak, M. M. 1975, ApJ, 202, 58

Manso Sainz, R. & Landi Degl'Innocenti, E. 2002, A&A, 394, 1093

Manso Sainz, R. & Trujillo Bueno, J. 2003, Phys. Rev. Letters, Vol. 91, 111102-1

Trujillo Bueno, J. 1999, in *Solar Polarization*, eds. K.N. Nagendra & J.O. Stenflo, Kluwer Academic Publishers, 73

Trujillo Bueno, J. 2001, in *Advanced Solar Polarimetry: Theory, Observation and Instrumentation*, ed. M. Sigwarth, ASP Conf. Series, Vol. 236, 161

Trujillo Bueno, J. 2003, in *Stellar Atmosphere Modeling*, eds. I. Hubeny, D. Mihalas & K. Werner, ASP Conf. Series, Vol. 288, 551

Trujillo Bueno, J., & Landi Degl'Innocenti, E. 1997, ApJ, 482, L183

Trujillo Bueno, J., Casini, R., Landolfi, M. & Landi Degl'Innocenti, E. 2002*a*, ApJ, 566, L53

Trujillo Bueno, J., Landi Degl'Innocenti, E., Collados, M., Merenda, L. & Manso Sainz, R. 2002*b*, Nature, 415, 403

Trujillo Bueno, J., Shchukina, N. & Asensio Ramos, A. 2004, Nature, 430, 326

Western, L. R. & Watson, W. D. 1983a, ApJ, 268, 849

Western, L. R. & Watson, W. D. 1983b, ApJ, 275, 195

Western, L. R. & Watson, W. D. 1984, ApJ, 285, 158